2014 IEEE NINTH INTERNATIONAL CONFERENCE ON INTELLIGENT SENSORS, SENSOR NETWORKS AND INFORMATION PROCESSING (ISSNIP)
SYMPOSIUM ON COMPUTATIONAL INTELLIGENCE
SINGAPORE, 21–24 APRIL 2014

Image Deblurring for Navigation Systems of Vision Impaired People Using Sensor Fusion Data

Nimali Rajakaruna[1], Chamila Rathnayake[2], Kit Yan Chan[3], Iain Murray[4]
Department of Electrical and Computer Engineering
Curtin University
Perth, Western Australia
nimali.rajakaruna@curtin.edu.au[1], r.m.rathnayake@postgrad.curtin.edu.au[2], kit.chan@curtin.edu.au[3], I.Murray@curtin.edu.au[4]

***Abstract*— Image deblurring is a key component in vision based indoor/outdoor navigation systems; as blurring is one of the main causes of poor image quality. When images with poor quality are used for analysis, navigation errors are likely to be generated. For navigation systems, camera movement mainly causes blurring, as the camera is continuously moving by the body movement. This paper proposes a deblurring methodology that takes advantage of the fact that most smartphones are equipped with 3-axis accelerometers and gyroscopes. It uses data of the accelerometer and gyroscope to derive a motion vector calculated from the motion of the smartphone during the image-capturing period. A heuristic method, namely particle swarm optimization, is developed to determine the optimal motion vector, in order to deblur the captured image by reversing the effect of motion. . Experimental results indicated that deblurring can be successfully performed using the optimal motion vector and that the deblurred images can be used as a readily approach to object and path identification in vision based navigation systems, especially for blind and vision impaired indoor/outdoor navigation. Also, the performance of proposed method is compared with the commonly used deblurring methods. Better results in term of image quality can be achieved. This experiment aims to identify issues in image quality including low light conditions, low quality images due to movement of the capture device and static and moving obstacles in front of the user in both indoor and outdoor environments. From this information, image-processing techniques to will be identified to assist in object and path edge detection necessary to create a guidance system for those with low vision.**

Keywords—image deblurring; inertial sensors; vision impaired navigation; particle swarm optimization

I. INTRODUCTION

This work forms a part of a development project for real time local navigation (indoor and outdoor) based on edge detection techniques using hand held devices (e.g. smartphones). This research focuses on the challenges that have to be faced in path finding using image processing and edge detection, such as poor lighting conditions, shadow conditions, low quality images due to movement of the capture device and static and moving obstacles in front of the user. Under these conditions it's difficult to detect edges of sidewalks, corridors, path edges, stairways, pedestrian crossing and obstacles. This paper proposes a novel method to analyze the issues related to image blurring.

Image bluriness is one of the primary causes of poor image quality in image acquisition and can significantly degrade the structure of sharp images. Atmospheric turbulences, out-of-focus and the motion of camera or scene would cause the blur. One of the most common reasons for image degrading is camera shake blur when the light conditions are poor as the exposure time under poor lighting conditions is high. The camera shake is high in human way finding application as there is significant movement with the use of a body mounted camera. Although faster shutter speeds would reduce the motion blur that can increase camera noise and availability of high-speed cameras in mobile phones and embedded systems is very low.

Real time object detection and path identification using edge detection is a significant component of image processing in way finding systems for vision-impaired people [1]. Low-resolution images are used to reduce the complexity and computational demands as way finding systems usually have to be implemented as an embedded system. The discontinuities of detected edges can be increased if the edges are detected with the bluriness of the image. When too many unnecessary discontinuities are generated, errors in object detection or path identification are likely to be produced, thereby creating potential dangers for vision-impaired people.

Recent technologies in mobile devices enable the estimation of the PSF using the embedded inertial sensors. While the 3-axis accelerometer gives the linear motion, the 3-axis gyroscope gives the rotary motion. However, the main challenge in using the accelerometer to compute motion is the noise accumulation when performing integration of the accelerometer signal to compute velocity and displacement [2], [3]. Also, an appropriate PSF for effective deblurring is difficult to be generated, as the exposure time is mostly short. Hence, it reduces the deblurring performance when an inappropriate PSF is used.

In this paper, a non-blind deblurring methodology is proposed, where the PSF is determined based on the 3-dimensional linear motion of the scene with respect to the camera. A heuristic method, namely particle swarm optimization [18], is developed to determine optimal

978-1-4799-2843-9/14/$31.00 ©2014 CROWN

parameters of the PSF, in order to further improve the deblurring performance. Experimental results show that the proposed method can improve the image quality of the deblurred images. Significant improvement may also be achieved when compared with the commonly used deblurring methods [10] such as blind deconvolution, Wiener filter, Lucy-Richardson method and the regularized filter.

In Section II, previous work related to image deblurring with and without using inertial sensor data are discussed. Section III describes the proposed deblurring method. Section IV presents the PSF determined by the proposed method and presents the results obtained by proposed method and other commonly used deblurring methods. Comparison with the proposed method and the other tested methods are also given. The conclusion and future work are given in Section V.

II. Related Work

Image deblurring has recently received significant attention and has been a continuing problem in the image processing and computer vision fields. Image deblurring can be classified into two types, blind and non-blind deconvolution. Deblurring is more difficult and ill-posed problem when the blur kernel is unknown, which is classified as blind deconvolution. When the blur kernel is known all practical solutions can be stronger than the prior information is unknown about the kernel. These techniques are classified as non-blind deconvolution. Image deblurring is a combination of point spread function (PSF) and non-blind deconvolution. For further literature in this area, we refer the survey article by Kundar and Hatzinakos [4].

The majority of the approaches carried out in deblurring requires minimum of two images of the same scene. Rav- Acha and Peleg [5] used the information in two motion blurred images, while Lu et al. [6] used a pair of images, one blurry and one noisy, to facilitate capture in low light conditions. But capturing two images in the same scene is not suitable in the area of way finding due to the real time constraints.

Fergus et al. [7] discuss a method on removing camera shake using a single image. This solution identifies the camera motion using an initial kernel estimation, which requires a region without saturation effects. Qi et al. [8] propose a method using a unified probabilistic model of both blur kernel estimation and deblurred image restoration. Both these methods require complex computational processing which is not suitable for devices with limited processor and memory resources.

Many devices, such as modern smartphones have in-built inertial sensors: gyroscopes and accelerometers. The use of inertial measurement unit (IMU) data to calculate the camera motion may be simpler than the above methods and some of the research already carried out in this area [9, 10, 11, 12]. Hyeoungho et al. [9] proposed a deblurring method using an integrated depth sensor and IMU sensor with the camera. The joint analysis of these three types of data is used for the better recovery of the real camera motion during the exposure time. This method requires intensive computations to be run on a laptop to control the depth sensor which is not feasible in the area of way finding. Horstmeyer et al. [10], Feng et al. [11] and Joshi et al. [12] discuss deblurring methods using the accelerometer and gyroscopic sensor data and have used DSLR camera, which is more expensive, and a set of sensors, and used an offline computer for image deblurring process.

Sanketi et al. [13] describe methods of anti-blur feedback for visually impaired users of Smartphone camera using the IMU sensor data. Primarily, this feedback is used for the camera stabilization and this is also another use of synchronized IMU data, which is useful in the area of image acquisition. Also similar to our work is that of Šindelář and Šroubek [14], which uses a smart phone with gyroscope to remove the camera shake blur. In the work presented in this paper, both gyroscope and accelerometer measurements are used to estimate the motion blur because there can be linear motion as well as rotation.

Because this research is based on way finding for vision-impaired people, the targetted walking speeds are in the order of 1.5 steps per second. Hence, the expected frame rate is in the order of 3-5 frames per second. It is expected that captured images will be of poor quality due to lighting conditions, blur and shadows.

III. Proposed Methodology

A. Camera Motion Blur

In general photography scenarios, the user tries to keep the camera as steady as possible. In this case the motion blur is minimal and most of deblurring techniques are targeting this kind of motion blur. However, in way finding applications, there is little control on the movement of the camera, and the result is a heavy motion blur. Therefore, knowing the camera motion is important so that it can be given as an input to the deblurring algorithm.

B. Inertial Sensors and Calibrations

The sensors used to estimate the movements of the camera are the accelerometer for linear motion and the gyroscope for rotary motion. However, the issues in using the accelerometer to compute the linear displacement are the gravity component present in accelerometer data [2], the drift caused by the double integral [3] and the fact that the initial velocity is unknown. Further, the gyroscope drift introduces an error when integrated to compute the angular displacement [3]. However, experiments have indicated that, for a period of 200 ms, the drift caused by the accelerometer integration is in the range of 0.1 mm once the static error is removed and proper filtering is used and the drift in the angular displacement is in the range of 1/1000°. 200 ms was considered as the exposure time of an image is generally below 100 ms [15].

Fig. 1 shows the linear and angular displacements computed from the accelerometer and gyroscope sensor data collected while the phone is kept stationary on top of a table. This indicates that once proper filtering is done to the sensor signals, the error caused by the drift can be neglected in the scenario considered.

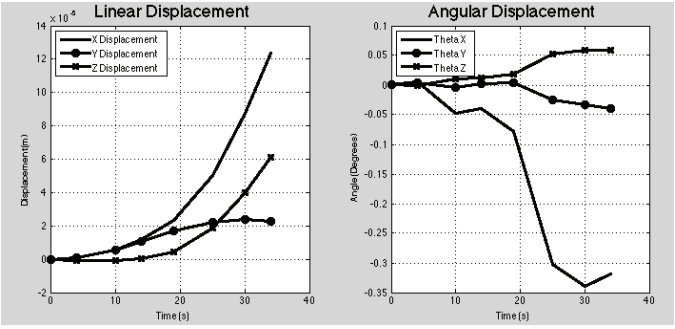

Fig. 1. Error in linear and angular displacements caused by the integration of sensor noise

C. Determination of PSF

The blurriness of an image may cause due to linear and angular movements of the camera with respect to the scene. If the camera is considered to be stationary, the scene can be considered as moving with respect to the camera. The blur function or the PSF will both on the plane of the scene and perpendicular to that. The component on the plane of the scene causes a linear blur while the perpendicular component causes a zooming effect. Both linear and rotary movements contribute to all these PSF components. Fig. 2 illustrates the placement of the scene w.r.t. the camera, the motion components of the camera and the velocity components of a point on the frame in interest having coordinates (a, b) w.r.t. the center of the frame. A frame parallel to the plane of the camera that is placed at a distance of l is of interest for this analysis as a plane at a fixed distance is always consider for deblurring. Coordinate system of the camera is taken as the coordinate system for this analysis. Table I shows the motion parameters of the camera and a point (a, b) on the frame as indicated in Fig. 1. However, as the contribution of linear velocity components, Vx, Vy and Vz, to the velocity of the point on the scene is very small compared to the contribution from angular velocity, 1 can be minimized to 2. Once the velocity components are computed using 1 or 2, 3-dimentional displacement components are computed by time integrating each velocity component for the period of exposure using trapezoid rule.

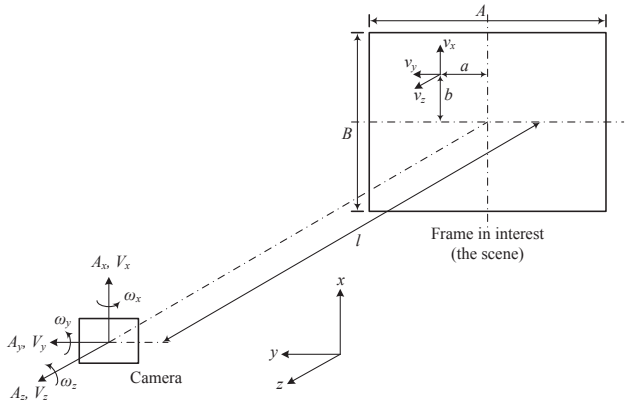

Fig. 2. Illustration of the scene with respect to the camera

$$\begin{aligned} vx &= -Vx + l\omega y + a\omega z \\ vy &= -Vy - l\omega x - b\omega z \\ vz &= -Vz - a\omega x + b\omega z \end{aligned} \quad (1)$$

$$\begin{aligned} vx &= l\omega y + a\omega z \\ vy &= -l\omega x - b\omega z \\ vz &= -a\omega x + b\omega z \end{aligned} \quad (2)$$

TABLE I. MOTION PARAMETERS OF THE CAMERA AND THE FRAME

Parameter	Value
A_x, A_y, A_z	Linear acceleration of camera along x, y and z axis
V_x, V_y, V_z	Linear velocity of camera along x, y and z axis
$\omega_x, \omega_y, \omega_z$	Angular velocity of camera along x, y and z axis
v_x, v_y, v_z	Linear velocity of frame w.r.t. camera along x, y and z axis

Now that the movement of a point within the exposure time is known, it has to be converted to pixel displacements. The challenge faced in this computation was that both sensor size and the focal length were unknown, as the vendors do not provide them. To overcome this problem, a practical measurement was taken to find the ratio B/l. It was also confirmend that $B/A = 3/4$ during this measurement. The values of A and B at the frame in interest were computed using the ratio B/l measured. If the resolution of the image is $m \times n$ $(m{:}\, n = 4{:}\, 3)$ the pixel size at the scene can be computed as A/m or B/n. From this, the total pixel displacements in x and y directions were computed and those are the dimensions of PSF matrix.

The next task was to compute the PSF matrix from the displacements computed. The challenge here was that the samples of x and y displacements (dx and dy) computed placed several columns and rows apart in the PSF matrix. Therefor, linear interpolation was used to fill the gap between those samples. Fig. 3 shows the algorithm used to derive the PSF from computed displacements on the plane of the scene. The movement along z-axis was not incorporated in this computation so that the zooming can be considered separately.

When an appropriate PSF is determined, the deblurring can be conducted on the blurred image and the image quality can be improved. To further improve the PSF on deblurring, the optimal alignment parameters namely *a, b* and *l* in equations (1) and (2) is necessary to be determined with respect to the image quality. The following section presents a commonly used heuristic method namely particle swarm optimization (PSO) [18, 20, 21] in order to determine the optimal alignment parameters. When the optimal alignment parameters are determined, optimal image quality can be obtained for the deblurred image.

```
SET x span to Total X axis displacement
SET y span to Total Y axis displacement
SET N to Total number of
points for i = 1:N do
if x_span > y_span
    Divide X into number of rows between
    previous x coordinate and next x
    coordinate
  Gradient M = (Y)/(X)
  Calculate corresponding y values using
  previous y and M
  for j = 0 : N do
    col=Round(y)
    row=Round(x)
    PSF(col,row) = PSF(col,row) + 1

  end else
    Divide Y into number of columns between
    previous y coordinate and next y
    coordinate
  Gradient M = (X)/(Y)
  Calculate corresponding x values using
  previous x and M
  for j = 0 : N do
    col=Round(y)
    row=Round(x)
    PSF(col,row) = PSF(col,row) + 1

end

end
```

Fig. 3. Illustration of the scene with respect to the camera

D. Optimization of PSF

The PSO consists of N_s particles, where the position of the *j*-th particle at the *g*-th generation is represented by:

$$P_j^g = \left(K_{j,1}^g, K_{j,2}^g, K_{j,3}^g\right), \tag{3}$$

where $K_{j,1}^g$, $K_{j,2}^g$, $K_{j,3}^g$ are represented by three alignment parameters namely *a*, *b* and *l* respectively. At the 1-*st* generation with *g*=1, all $K_{j,k}^g$, with *k*=1, 2, 3, are generated randomly within their operational ranges, given as

$K_{j,1}^g \in [a_{min}, a_{max}]$, $K_{j,2}^g[b_{min}, b_{max}]$, and $K_{j,2}^g[l_{min}, l_{max}]$.

All $K_{j,k}^g$, with *k*=1, 2, 3, are evaluated based on quality of the deblurring image which are determined using the image quality analyzer [19]. When g>1, each P_j^g are updated based on its velocity, $vel_{j,k}^g$, by the following formulation (4):

$$K_{j,k}^g = K_{j,k}^{g-1} + vel_{j,k}^g, \tag{4}$$

where

$$vel_{j,k}^g = C\left(v_{j,k}^{g-1} + \varphi_1.\gamma.\left(pbest_{j,k} - K_{j,k}^{g-1}\right) + \varphi_2.\gamma.\left(K_{j,k}^{g-1}\right)\right) \tag{5}$$

$pbest_j = \left[pbest_{j,1}, pbest_{j,2}, pbest_{j,3}\right]$, and

$gbest = [gbest_1, gbest_2, gbest_3]$;

$pbest_j$ denotes the best previous position of a particle recorded from the previous generation; *gbest* denotes the position of the best particle among all particles; γdenotes a random number in the range of [0,1]; *w* is an inertia weight factor; $\phi_1$and ϕ_2 are the acceleration constants [1]; and *C* denotes the constriction factor, that ensures the PSO converges [2], which is given by:

$C = \frac{2}{\left|2-\phi-\sqrt{\phi^2-4\phi}\right|}$, with $\phi = \phi_1 + \phi_1$and $\phi > 4$

The PSO utilizes $pbest_j$ and *gbest* to modify the current location of all $K_{j,k}^g$ in order to prevent them from moving in the same direction, but to converge gradually towards $pbest_i$ and $gbest$ [3]. To further refine the dynamic of $K_{j,k}^g$, $vel_{j,k}^g$is limited by a value, which was set as 10%–20% of its range. This limit is employed to avoid $K_{j,k}^g$ from flying past good solutions or exploring insufficient local solutions. The searching process of the PSO stops when it converges to the optimal alignment parameters with respect to the image quality defined in [19], where the optimal alignment parameters are denoted as

$$\overline{K}^{opt} = \left[K_{j,1}^{opt}, K_{j,2}^{opt}, K_{j,3}^{opt}\right].$$

IV. EXPERIMENTAL RESULTS

The PSF is derived using the method described in "Estimation of PSF" section was used to deblur an image captured with synchronized inertial sensor data while the camera is in motion. Fig. 4 shows the PSF estimated using recorded inertial sensor data for the center of the image and for the center of each quarter of the image. Fig. 5 shows the original image and deblurred images processed by the proposed method and the five commonly used deblurring methods [10] namely Blind Deconvolution, Wiener filter, Lucy-Richardson method, and regularized filter. The computed PSF was used in the deblurring methods except the blind deconvolution method, as PSF is not required in the blind deconvolution method. Regularized filter was used as the deblurrer in the proposed method (here in after referred to as PSO-Regularized technique) and was engaged with the optimal alignment parameters determined by the PSO discussed in "Optimization of PSF" subsection.

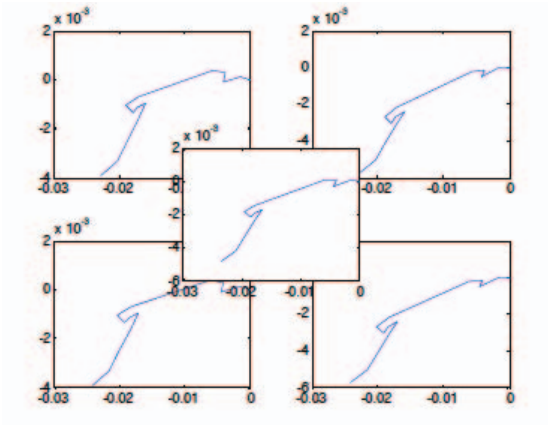

Fig. 4. PSF of different positions of image

Fig. 5. Images with different deblurring techniques. 1: Original image, 2: Blind Deconvolution 3: Wiener filter, 4: Lucy-Richardson method, 5: Regularized filter, and 6: proposed method (started from the top left hand side to the bottom right hand side)

This experiment was carried out using a Sony Xperia TX smartphone and the images and sensor data were captured while the camera in motion to simulate the navigation. The standard deblurring and edge detection techniques were applied and tested using MATLAB 2013R. The average computational time for the total processing over the different techniques was measured as 800 milliseconds.

Fig. 5 clearly shows that the deblurred images generated by the five deblurred methods are generally better than the original blurred image. However, it is difficult to evaluate the image quality by observing solely the deblurred images. An image quality measure defined by Mittal et al. [19] is used to evaluate the image quality of the deblurred image, where the image quality measure is effective to predict the quality of distorted images with little prior knowledge of the images or their distortions. Table II shows that quality score evaluated for the original image is the poorest. The quality scores obtained by the blind deconvolution method, Wiener filter and Lucy-Richardson method are similar which are poorer than those obtained by the regularized filter and the PSO-Regularized technique. Among the five tested deblurring methods, the PSO-Regularized technique could obtain the best quality score.

To further illustrate the performance of the PSO-Regularized technique, Tabel II shows the relative improvements when each of the four tested methods are compared with the PSO-Regularized technique, where the relative improvement is the difference between the results obtained by the PSO-Regularized technique and the other tested method, divided by the result obtained by the other tested method. They indicate the relative differences between the results obtained by the PSO-Regularized technique and those obtained by the four tested methods. For the image quality scores, the PSO-Regularized technique obtained improvements with more than 10% relatively to Blind Deconvolution, Wiener filter, and Lucy-Richardson method. Also, the PSO-Regularized technique obtained an improvement with more than 5% relative to the Regularized filter. These results further indicate the effectiveness of the PSO-Regularized technique.

TABLE II. QUALITY OF THE ORIGINAL AND PROCESSED IMAGES

Image	Quality Score	Improvement relatively to PSO-Regularised technique (Percentage)
Original	19.8734	14.214943
Blind deconvolution	19.1981	10.333908
Wiener filter	19.4946	12.037931
Lucy-Richardson method	19.2360	10.551724
Regularized filter	18.3384	5.393103
PSO-Regularized technique	17.4	Nil

V. CONCLUSION AND FUTURE WORK

In this paper, a novel method is proposed to determine the optimal PSF using the information from built-in inertial sensors of smartphones, in order to improve the image quality of the deblurred image. A heuristic method, particle swarm optimization, is developed to optimize the parameters of the PSF. Hence, deblurring can be effectively performed using the optimal PSF. Experimental results show that the proposed method, the PSO-Regularized technique, can improve the image quality of the deblurred images. Also, significant improvement can be achieved when compared with the commonly used deblurring filters including blind deconvolution, Wiener filter, Lucy-Richardson method and the Regularized filter.

One of the limitations of the PSO-Regularized technique is the sensor accuracy and the sensor noise, which causes the ringing artifacts. This will be a critical factor in edge detection for navigation. The primary focus of this research is way finding for vision- impaired people and hence the noise level should be reduced and the computational cost should be within 100 ms. This will be a topic of future work which is to introduce an optimized novel algorithm for deblurring using an inertial sensor data based PSF. Additionally, approaches based on neural networks [20, 23] will be developed in order to generate the deblurring kernels based on the trajectories of camera motion.

REFERENCES

[1] Rajakaruna N., Murray I., "Edge detection for Local Navigation System for Vision Impaired People Using Mobile Devices", International Conference on Mathematical Sciences & Computer Engineering, Malaysia, 29-30 Nov. 2012.

[2] K. Abhayasinghe and I. Murray. (2012, Nov.). "A novel approach for indoor localization using human gait analysis with gyroscopic data," in

Third International Conference on Indoor Positioning and Indoor Navigation (IPIN2012) [Online], Sydney, Australia, 2012. Available: http://www.surveying.unsw.edu.au/ipin2012/proceedings/submissions/22_Paper.pdf [Mar. 5, 2013].

[3] D. Sachs. Google Tech Talk, Topic: "Sensor Fusion on Android Devices: A Revolution in Motion Processing." [On-Line], Aug. 2, 2010. Available: http://www.youtube.com/watch?v=C7JQ7Rpwn2k [Oct. 27, 2011].

[4] Kundur, D.; Hatzinakos, D., "Blind image deconvolution," Signal Processing Magazine, IEEE , vol.13, no.3, pp.43,64, May 1996

[5] Rav-Acha, A., & Peleg, S. 2005. Two motion blurred images are better than one. Pattern Recognition Letters 26, 311–317.

[6] Yuan, Lu, Sun, Jian, Quan, Long, & Shum Heung-Yeung. (2007). Image deblurring with blurred/noisy image pairs. Paper presented at the ACM SIGGRAPH 2007 papers, San Diego, California.

[7] Fergus, Rob, Singh, Barun, Hertzmann, Aaron, Roweis, Sam T., & Freeman, William T. (2006). Removing camera shake from a single photograph. Paper presented at the ACM SIGGRAPH 2006 Papers, Boston, Massachusetts.

[8] Shan, Qi, Jia, Jiaya, & Agarwala, Aseem. (2008). High-quality motion deblurring from a single image. Paper presented at the ACM SIGGRAPH 2008 papers, Los Angeles, California.

[9] Hyeoungho, Bae, Fowlkes, C. C., & Chou, P. H. (2013, 15-17 Jan. 2013). Accurate motion deblurring using camera motion tracking and scene depth. Paper presented at the Applications of Computer Vision (WACV), 2013 IEEE Workshop on.

[10] Horstmeyer, Roarke, (2010), Camera Motion Tracking for De-blurring and Identification. MIT Media Lab MAS 863 Final Project.

[11] Feng , JIN, Tian,LI. Digital image stabilization system based on inertial measurement module School of Automation, Beijing Institute of Technology, Beijing 100081, China.

[12] Joshi, Neel, Kang, Sing Bing, Zitnick, C. Lawrence, & Szeliski, Richard. (2010). Image deblurring using inertial measurement sensors. Paper presented at the ACM SIGGRAPH 2010 papers, Los Angeles, California.

[13] Sanketi, Pannag R., & Coughlan, James M. (2010). Anti-blur feedback for visually impaired users of smartphone cameras. Paper presented at the Proceedings of the 12th international ACM SIGACCESS conference on Computers and accessibility, Orlando, Florida, USA.

[14] Šindelář O, Šroubek F; Image deblurring in smartphone devices using built-in inertial measurement sensors. J. Electron. Imaging. 0001;22(1):011003-011003.

[15] A. Davis, (2012, Apr. 24). "What are the shutter speed and ISO ranges for the iPhone 4S camera?" [Weblog entry]. Ask Different. Available:http://apple.stackexchange.com/questions/49556/what-are-theshutter-speed-and-iso-ranges-for-the-iphone-4s-camera [Mar. 5, 2013].

[16] R.C. Eberhart and Y. Shi, Comparison between genetic algorithms and particle swarm optimization, in Evolutionary Programming VII. New York: Springer-Verlag, LNCS, vol. 1447, pp. 611-616, 1998.

[17] F. Bergh and A.P. Engelbrecht, A study of particle swarm optimization particle trajectories, Information Sciences, vol. 176, no. 8, pp.937-971, 2006.

[18] K.E. Parsopoulos and M.N. Vrahatis, On the computation of all global minimizers through particle swarm optimization, IEEE Transactions on Evolutionary Computation, vol. 8, no. 3, pp. 211-224, 2004.

[19] Mittal, A., Soundararajan, R. & Bovik, A. C. (2013). Making a "Completely Blind" Image Quality Analyzer. IEEE Signal Process. Lett., 20, 209-212.

[20] CK Kwong, KY Chan, H Wong, An empirical approach to modelling fluid dispensing for electronic packaging, The International Journal of Advanced Manufacturing Technology, vol. 34 no 1-2, 111-121, 2007.

[21] SH Ling, CW Yeung, KY Chan, HHC Iu, FHF Leung, A new hybrid particle swarm optimization with wavelet theory based mutation operation, Proceedings of IEEE Congress on Evolutionary Computation, pp. 1977-1984 2007.

[22] KY Chan, TS Dillon, J Singh, E Chang, Neural-network-based models for short-term traffic flow forecasting using a hybrid exponential smoothing and Levenberg–Marquardt algorithm, IEEE Transactions on Intelligent Transportation Systems, vol. 13, no. 2, pp. 644-654, 2012.